

WUB 98-27
HLRZ1998-54

The Pion-Nucleon σ -Term with Dynamical Wilson Fermions

SESAM Collaboration

S. Güsken^a, P. Ueberholz^a, J. Viehoff^a
N. Eicker^b, P. Lacock^b, T. Lippert^a, K. Schilling^{a,b}, A. Spitz^b, T. Struckmann^a

^a *Bergische Universität Wuppertal, Fachbereich Physik, 42097 Wuppertal, Germany*

^b *HLRZ Forschungszentrum Jülich, and DESY, Hamburg, 52425 Jülich, Germany*

Abstract

We calculate connected and disconnected contributions to the flavour singlet scalar density amplitude of the nucleon in a full QCD lattice simulation with $n_f = 2$ dynamical Wilson fermions at $\beta = 5.6$ on a $16^3 \times 32$ lattice. We find that both contributions are of similar size at the light quark mass, in contrast to the outcome of previous quenched simulations. The full amplitude, connected plus disconnected, is seen to remain close to the quenched number. We arrive at the estimate $\sigma_{\pi N} = 18(5)$ MeV. Its smallness is directly related to the apparent decrease of u , d quark masses when unquenching QCD lattice simulations. The y parameter can be estimated from a semi-quenched analysis, in which there are no strange quarks in the sea, the result being $y = 0.59(13)$.

1 Introduction

The pion-nucleon σ -term is defined as the flavour singlet scalar density amplitude of the nucleon, multiplied by the light quark mass m_{ud}

$$\sigma_{\pi N} = m_{ud} \langle N | \bar{u}u + \bar{d}d | N \rangle \quad , \quad m_{ud} = 1/2(m_u + m_d) . \quad (1)$$

Our motivation to study this quantity in a full QCD simulation is twofold. First of all $\sigma_{\pi N}$ provides a direct measure of the explicit chiral symmetry breaking in QCD. A comparison of its experimental value with a (first principles) QCD calculation is therefore of great importance for the understanding of the chiral properties of the strong interaction. Secondly, the scalar density amplitude receives contributions from both connected and disconnected (vacuum polarization) diagrams. This is shown in fig.1. In a flavour singlet combination, such as $\sigma_{\pi N}$, the latter are simply added. Therefore, one expects sizeable contributions from those processes, which most likely will depend on the details of the vacuum structure. Given this, the pion-nucleon σ -term provides an ideal opportunity to disclose the impact of sea quarks on nucleon properties.

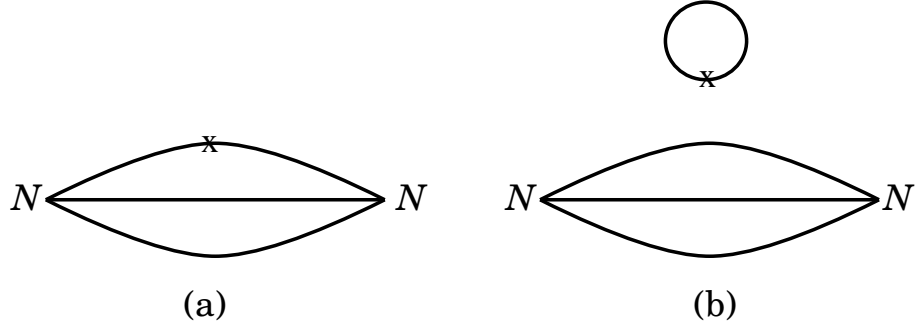


Figure 1: *Connected (a) and disconnected (b) contributions to the scalar density amplitude of a nucleon. Please note that all quark lines, including the quark loop, are connected by infinitely many gluon lines and virtual quark loops.*

On the other hand the determination of the experimental value of $\sigma_{\pi N}$ is by no means straightforward as it requires quite a bit of theoretical input. For instance it implies the use of pion-nucleon scattering data at the unphysical Cheng-Dashen point. A careful analysis of the extrapolation procedures has been performed by Gasser, Leutwyler and Sainio[1] by means of dispersion relations and chiral perturbation theory. They found $\sigma_{\pi N} \simeq 45$ MeV. A consistent value, $\sigma_{\pi N} = 48 \pm 10$ MeV, has been obtained more recently in the framework of heavy baryon chiral perturbation theory by the authors of ref.[2].

Additional information can be drawn from the baryon octet mass splittings. The flavour octet quantity

$$\sigma_0 = \frac{m_u + m_d}{2} \langle N | \bar{u}u + \bar{d}d - 2\bar{s}s | N \rangle \quad (2)$$

is related to $\sigma_{\pi N}$ by

$$\sigma_{\pi N} = \frac{\sigma_0}{1 - y}, \quad y = \frac{2\langle N | \bar{s}s | N \rangle}{\langle N | \bar{u}u + \bar{d}d | N \rangle}. \quad (3)$$

The analysis of the baryon octet mass splittings in first order chiral perturbation theory yields $\sigma_0 \simeq 25$ MeV. It has been pointed out however[3], that corrections due to terms $\propto m_s - 1/2(m_u + m_d)^2$ may enhance this value on a (20 – 30)% level. Relating these findings with the results of the πN scattering analysis leads to the estimate $y \simeq 0.2 – 0.4$. This implies that strange quark loops decrease the value of σ_0 by 20 – 40%. Naively, i.e. under the assumption of an approximate $SU(3)$ flavour symmetry of the disconnected parts of the nucleon scalar density, one would expect light quark loops to contribute similarly to the pion-nucleon σ -term.

$\sigma_{\pi N}$ as well as y have been studied recently in quenched lattice simulations by Fukugita et al.[4] and Dong et al.[5]. Both calculations find a value for $\sigma_{\pi N}$ consistent with the ‘experimental’ results quoted above, and a rather large ratio $\langle N | \bar{u}u + \bar{d}d | N \rangle_{disc} / \langle N | \bar{u}u + \bar{d}d | N \rangle_{con} \simeq 2/1$.

Furthermore, ref.[4] estimates $y = 0.66(15)$. Given the value of 2 : 1 for the ratio of

disconnected to connected contributions, this is exactly the value one would expect from the assumption of flavour symmetry of the disconnected contributions. Such a find appears plausible since the quenched QCD vacuum is not sensitive to quark flavour nor mass.

The authors of ref.[5] on the other hand find a much smaller value, $y = 0.36(3)$. But this is mostly due to their use of phenomenologically inspired ansätze for the extrapolation in the quark mass and for the renormalization of disconnected contributions. We will come back to this point later. Moreover, their data sample being very limited, one might have doubts on the reliability of their error analysis.

Apart from this, it is by no means obvious that quenched lattice simulations are at all suited to yield sound first principle QCD predictions for $\sigma_{\pi N}$ and y . For the quenched approximation neglects internal quark loops in the vacuum field configurations. As sea quark loops are essential in the calculation of disconnected contributions, the quenched approximation appears to be inconsistent and might introduce a serious systematic bias to $\sigma_{\pi N}$ and y .

It is therefore of utmost importance to study these quantities in full QCD lattice simulations. Apart from the issue of the numerical value of $\sigma_{\pi N}$ one might learn about the physics of sea quarks in QCD from the relative weight of disconnected to connected contributions and the amount of flavour symmetry breaking in the disconnected sector.

We emphasize that the size of the y parameter is determined by these quantities: a large ratio of disconnected to connected parts and a high degree of symmetry breaking impose a low value on y .

The calculation of disconnected correlations functions in lattice QCD requires a high statistics of gauge field configurations, since such correlators receive contributions only from vacuum fluctuations. Even with a ‘state of the art’ statistics of $O(200)$ configurations one needs elaborate analysis techniques to enhance the signal to noise ratio. Previous exploratory full QCD simulations [6, 7] have therefore not been sensitive enough to resolve a possible unquenching effect.

In this paper we present the results of a full QCD lattice simulation with $n_f = 2$ quark flavours of (mass degenerate) Wilson fermions at $\beta = 5.6$ and a lattice volume of $n_s^3 \times n_t = 16^3 \times 32$ points. This corresponds to a lattice cutoff $a_\rho^{-1} \simeq 2.3\text{GeV}$ and a spatial length $L \simeq 1.4\text{fm}$. We have generated 200 statistically independent vacuum configurations at each of our 4 values of the sea quark mass, which correspond to $m_\pi/m_\rho = 0.833(3), 0.809(15), 0.758(11)$ and $0.686(11)$. Details of the simulation as well as the analysis of the light hadron spectrum can be found in [8].

The paper is organized as follows. In chapter 2 we will define the lattice correlators and explain our methods to extract the connected and the disconnected scalar density amplitudes of the nucleon. In chapter 3 the raw results are presented and the quality of our signals as they emerge from different analysis methods is discussed. The extrapolation to light quarks is performed in chapter 4. Here we also obtain our results for $\sigma_{\pi N}$ and y . Finally, summary and conclusions are given in chapter 5.

2 Analysis Setup

2.1 Ratio Methods

In order to optimize the signal to noise ratio and to study the systematics of different procedures we have applied several analysis methods both to the connected and to the disconnected parts of the scalar density matrix element.

2.1.1 Global Summation Method

The standard procedure is to consider the ratio[9]

$$R^{SUM}(t) = \frac{\sum_{\vec{x}} \langle N^\dagger(\vec{0}, 0) \sum_{\vec{y}, y_0} [\bar{q}q](\vec{y}, y_0) N(\vec{x}, t) \rangle}{\sum_{\vec{x}} \langle N^\dagger(\vec{0}, 0) N(\vec{x}, t) \rangle} - \langle \sum_{\vec{y}, y_0} [\bar{q}q](\vec{y}, y_0) \rangle. \quad (4)$$

N denotes an interpolating operator for the nucleon. With the help of the generating functional formalism of the path integral, and using the Feynman-Hellmann theorem, one obtains

$$R^{SUM}(t) = A + \langle N | \bar{q}q | N \rangle t, \quad (5)$$

provided the nucleon is in its ground state. Naively one would expect this requirement to hold at large time distances t . However, due to the summation over all time positions of $\bar{q}q$ in eq.4, R^{SUM} might even then be contaminated by nucleon excitations. Furthermore, the ratio receives contributions from quark loops at distances $y_0 \gg t$. Those do not add substantially to the signal, but, especially for the disconnected part, might enhance the noise. It is therefore advantageous to undo the summation over y_0 by evaluating the signals at definite values y_0 , in the range $0 \ll y_0 \ll t$.

2.1.2 Plateau Density Method

The local density ratio

$$R^{PLA}(t, y_0) = \frac{\sum_{\vec{x}} \langle N^\dagger(\vec{0}, 0) \sum_{\vec{y}} [\bar{q}q](\vec{y}, y_0) N(\vec{x}, t) \rangle}{\sum_{\vec{x}} \langle N^\dagger(\vec{0}, 0) N(\vec{x}, t) \rangle} - \langle \sum_{\vec{y}} [\bar{q}q](\vec{y}, y_0) \rangle \quad (6)$$

allows for an isolation of the proton ground state with respect to both t and y_0 . Its asymptotic time dependence can be evaluated in the transfer matrix formalism, without recourse to the Feynman-Hellmann theorem. For $0 \ll y_0 \ll t$ the ratio becomes independent of t and y_0 , and one obtains¹

$$R^{PLA}(t, y_0) = \langle N | \bar{q}q | N \rangle. \quad (7)$$

¹This form is valid for an infinitely extended lattice in time.

Thus, the ground state signature of R^{PLA} is a plateau instead of a linear rise. The height of the plateau will tell us about the scalar density nucleon matrix element.

We will demonstrate below that this method works well for the connected parts. However, one loses the advantage to gain statistics by summing over y_0 , which is a crucial issue for the disconnected part. For the calculation of the latter we have therefore decided to use a slightly modified technique which still accumulates data with respect to y_0 , but in a region characterized by ground state dominance of the signals.

2.1.3 Plateau Accumulation Method

The plateau accumulation method (PAM) combines the advantages of the global summation and of the plateau density techniques. It is defined by

$$R^{PAM}(t, \Delta t_0, \Delta t) = \sum_{y_0=\Delta t_0}^{t-\Delta t} R^{PLA}(t, y_0) , \quad (8)$$

with $1 \leq \Delta t, \Delta t_0 \leq t$. The asymptotic time dependence is given by

$$R^{PAM}(t, \Delta t_0, \Delta t) = \langle N | \bar{q}q | N \rangle (t - \Delta t - \Delta t_0) . \quad (9)$$

We have evaluated R^{PAM} for several values of Δt_0 and Δt . Within our statistical precision (200 gauge configurations) all results are consistent. In the final analysis we have therefore used $\Delta t_0 = \Delta t = 1$.

2.2 Numerical Evaluation

2.2.1 Connected Contributions

We compute the numerator of eq.4 (summation method) with the standard insertion technique [9]. This method is advantageous if one has to sum over all time positions y_0 . The additional effort, on top of the standard quark propagator calculation, is just to compute a modified quark propagator $\tilde{\Delta}(x, 0)$, defined as the solution to

$$M\tilde{\Delta}(x, 0) = \Delta(x, 0) . \quad (10)$$

Here M is the fermion matrix and Δ the quark propagator. Graphically, the modified quark propagator corresponds to the quark line with a cross in fig. 1a.

The standard insertion technique can be in principle applied also to the numerator of eq.6 (plateau method). However, as one avoids the summation over y_0 in this case, one would have to solve eq.10 n_t times. Instead, we use the advanced insertion technique proposed by Martinelli and Sachrajda[10]. Here, one keeps the nucleon sink and source at the largest possible time separation², and computes an advanced propagator by solving

²For (anti)periodic boundary conditions, the largest possible time distance is $n_t/2$.

the equation

$$\mathbf{M} \{ N(0) \xrightarrow{\substack{y \\ x}} N(x) \} = N(0) \xrightarrow{\substack{y \\ x}} N(x) . \quad (11)$$

Note that the r.h.s. is just a combination of standard quark propagators. The 3-point correlation is then given by the product of the advanced and the standard quark propagator. The position in time, y_0 , of the quark density $\bar{q}q$ is not fixed here and can be varied without additional cost.

2.2.2 Disconnected Contributions

The determination of the quark loop contributions to the scalar density matrix element requires the calculation of the trace of the quark propagator

$$L(y_0) = \sum_{\vec{y}, \alpha, a} [\bar{q}q](\vec{y}, y_0, \alpha, a; \vec{y}, y_0, \alpha, a) = Tr \Delta(y_0; y_0) . \quad (12)$$

α and a denote Dirac and colour degrees of freedom. An exact determination of L with conventional Krylov subspace methods would be prohibitively expensive since one would have to apply such an algorithm $n_s^3 \times n_t$ times. Instead one has to rely on approximate methods like the volume source technique[11] and the stochastic estimator technique with Gaussian[12] and with Z_2 [13] noise. The latter allow to control the accuracy of the estimator on each gauge configuration.

It has been demonstrated recently[14] that the stochastic estimator technique with (complex) Z_2 noise is superior for our lattice setup. Therefore we used this method here, albeit with small modifications which allow for the determination of

$$L(y_0, \beta', \beta) = \sum_{\vec{y}, a} \Delta(\vec{y}, y_0, a, \beta'; \vec{y}, y_0, a, \beta) , \quad (13)$$

where the Dirac indices are not contracted. Thus, the results can be re-used to calculate vacuum loops other than scalars. For completeness we sketch the relevant formulae of this *spin explicit method* here.

On a given configuration and for each estimate we choose N_E complex Z_2 random vectors $\eta(\vec{y}, y_0, a, \alpha)$, with $n_s^3 \times n_t \times 4 \times 3$ entries. Each component of η has the properties

$$\eta^*(i)\eta(i) = 1 \quad , \quad \langle \eta^*(i)\eta(j) \rangle = 0 \text{ for } i \neq j . \quad (14)$$

The brackets of the right equation denote the average over (infinitely many) stochastic estimates. From η we compose 4 *spin explicit* random vectors

$$\eta^\beta(\vec{y}, y_0, a, \alpha) = \eta(\vec{y}, y_0, a, \alpha)\delta_{\alpha, \beta} \quad , \beta = 0, 1, 2, 3 . \quad (15)$$

Note that there is no sum over α on the r.h.s. . The vector $\Delta\eta^\beta$ is then obtained as the solution to

$$M[\Delta\eta^\beta] = \eta^\beta . \quad (16)$$

According to eq.14, the product

$$P(t_0, \beta', \beta) = (\tilde{\eta}^{\beta', t_0})^\dagger \Delta\eta^\beta , \quad (17)$$

with $\tilde{\eta}^{\beta', t_0}(\vec{y}, y_0, a, \alpha) = \eta^\beta(\vec{y}, y_0, a, \beta) \delta_{y_0, t_0} \delta_{\alpha, \beta'}$

converges in the limit $N_E \rightarrow \infty$ on each gauge configuration to

$$\langle P(t_0, \beta', \beta) \rangle = L(y_0, \beta', \beta) . \quad (18)$$

In this work we have used 100 stochastic estimates per configuration. We have checked that this suffices to reach the asymptotic region.

3 Raw Data

Figs.2 and 3 display the ratios R^{SUM} and R^{PLA} of the connected contributions for our four quark masses. On each graph we show the data for both, the (scalar) interactions of the u and of the d quarks of the proton.

Note that R^{PLA} is plotted in fig.3 as a function of the (time) position of the scalar interaction y_0 . The time separation of proton sink and source is fixed at $t = 16$.

All ratios exhibit clear signals, even for the smallest value of our quark masses. From fits according to eqs.5 and 7 we extract the connected parts of the scalar density matrix element of the proton. These are listed in tab.1.

Method	κ	C_u	C_d	C_{u+d}
SUM	0.1560	2.08(4)	1.13(2)	3.21(5)
	0.1565	2.13(6)	1.18(4)	3.31(9)
	0.1570	2.26(11)	1.34(6)	3.60(17)
	0.1575	2.40(16)	1.46(13)	3.86(28)
PLATEAU	0.1560	1.92(5)	1.05(4)	2.98(8)
	0.1565	1.99(8)	1.15(5)	3.15(13)
	0.1570	2.08(13)	1.27(11)	3.35(24)
	0.1575	2.26(14)	1.33(11)	3.59(23)

Table 1: *Lattice results (unrenormalised) of the connected amplitude $C_q = \langle P(\kappa_{sea}) | \bar{q}q(\kappa_{sea}) | P(\kappa_{sea}) \rangle_{con.}$*

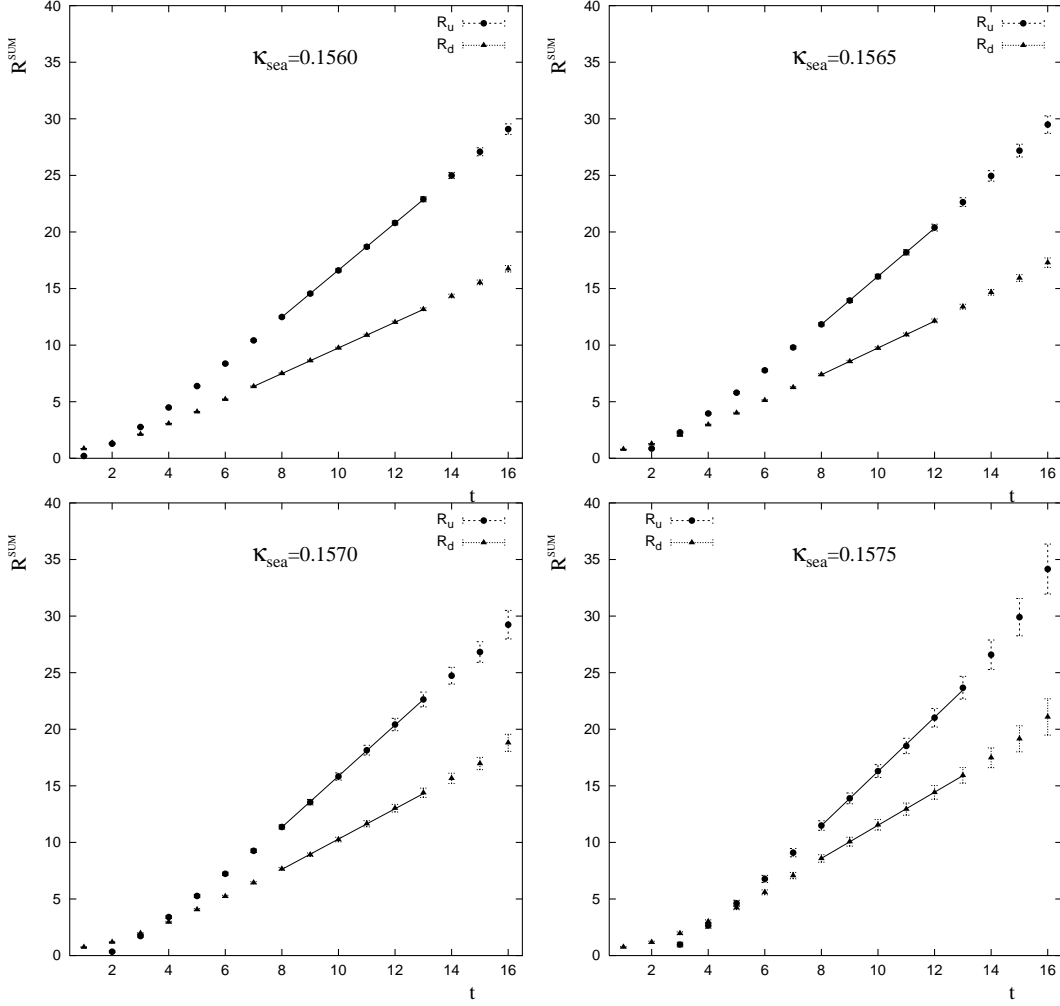


Figure 2: *Summation method:* The raw data R_u and R_d for the connected amplitudes $C_{u,d}$ at our sea quark masses. The fits (range and value) are indicated by solid lines.

Both methods yield consistent results within statistical errors. It appears however, that the summation method systematically leads to slightly larger values than the plateau method. We attribute this to a small contamination of the SUM results with excited proton contributions. We will therefore use the data from the plateau method for our final analysis.

The signals of the disconnected contributions are shown in fig. 4 for the summation method and in fig. 5 for PAM.

It turns out that the data analysed with the summation technique is quite noisy and the signal tends to vanish at the smallest quark mass. In contrast, PAM produces significantly improved signal to noise ratios over our entire range of quark masses.

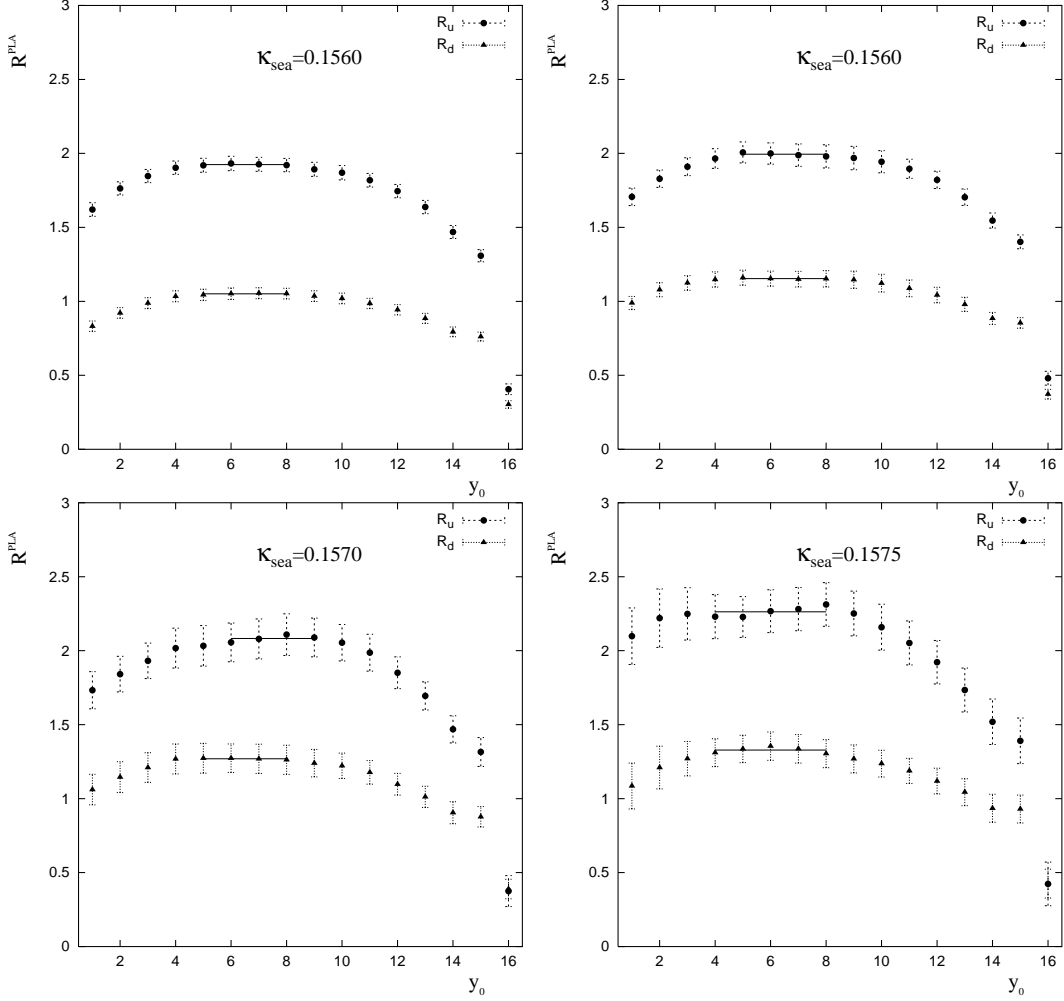


Figure 3: *Plateau method: The raw data R_u and R_d for the connected amplitudes $C_{u,d}$ at our sea quark masses. The fits (range and value) are indicated by solid lines.*

The outcome of the fits according to eqs.5 and 9 is compiled in tab.2. The PAM data are clearly superior with respect to statistical errors. It is gratifying to find the results of both methods to be compatible within (large) statistical uncertainties.

In tab.2 we have also included the raw data for the strange loop matrix element $\langle P|\bar{s}s|P\rangle$, which will be used for the determination of the y parameter. To obtain this data we held the loop quark fixed at the strange quark mass (c.f. [8]), and kept valence and sea quark masses degenerate under chiral extrapolation.

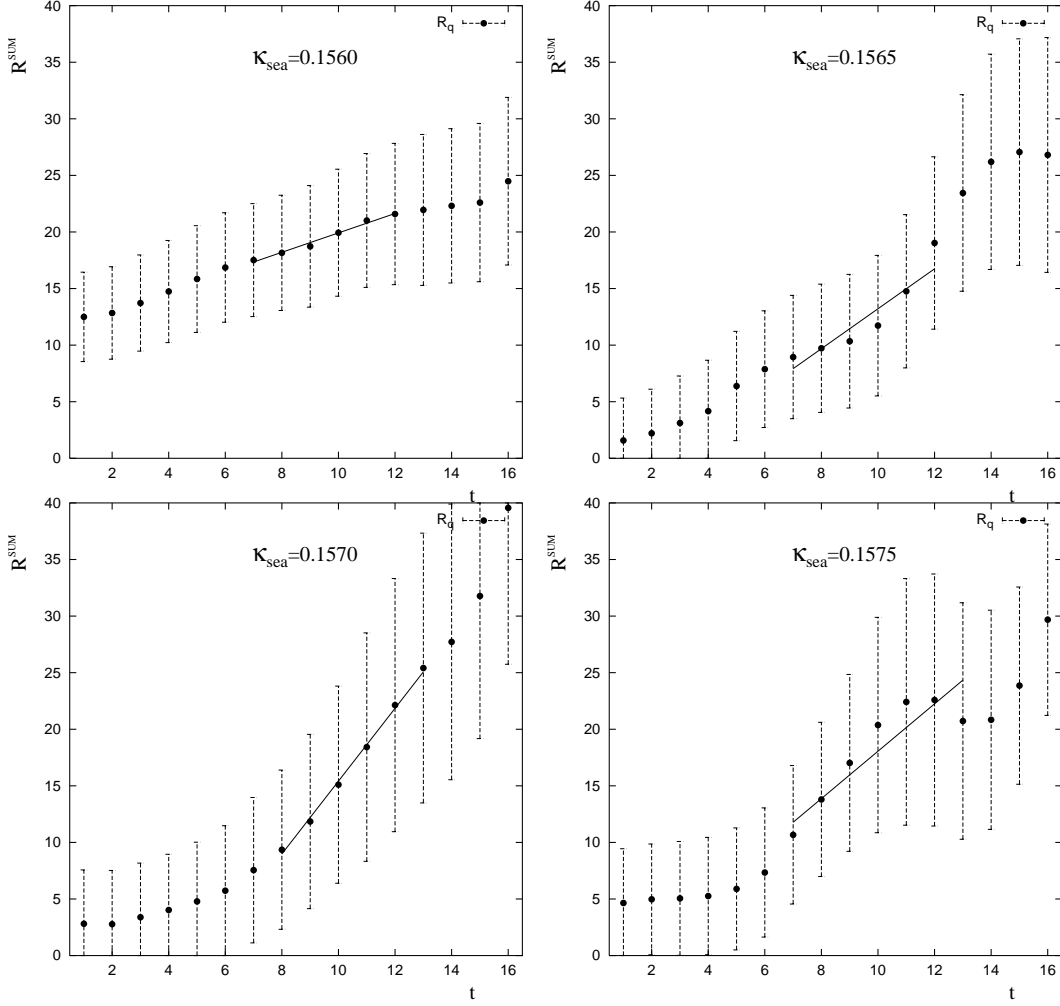


Figure 4: *Summation method: The raw data R_q for the disconnected amplitudes D_q at our sea quark masses. The fits (range and value) are indicated by solid lines.*

4 Physics Results

4.1 Pion-Nucleon σ -Term

Our procedure to obtain the physical value of $\sigma_{\pi N}$ is to extrapolate the results of tabs.1, 2 with respect to the quark mass to m_{ud} , and to multiply subsequently with the lattice cutoff a^{-1} and m_{ud} . Note that no renormalization is necessary, as $\sigma_{\pi N}$ is a renormalization group invariant quantity.

In fig.6 we display the extrapolations of the connected and disconnected amplitudes. Since the statistical quality of the disconnected contribution does not allow to resolve for

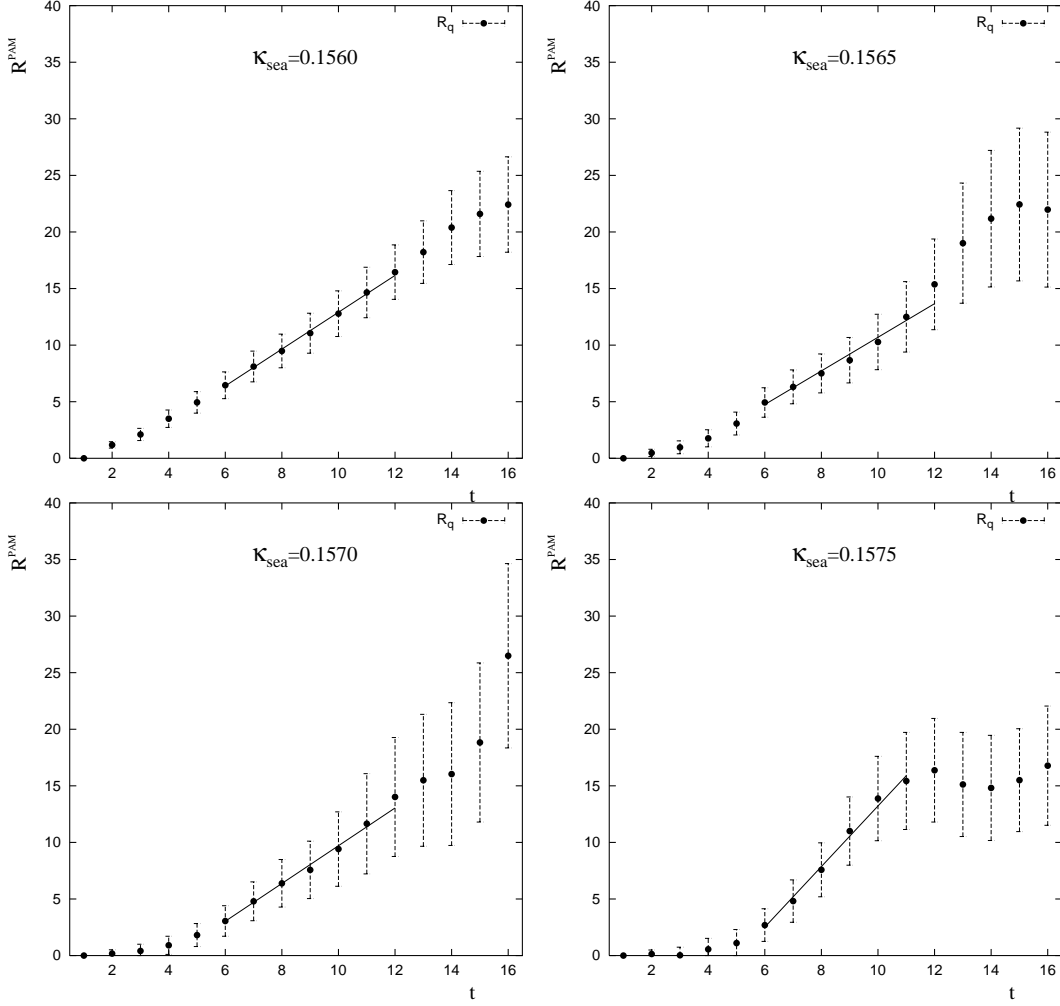


Figure 5: *PAM*: The raw data R_q for the disconnected amplitudes D_q at our sea quark masses. The fits (range and value) are indicated by solid lines.

higher orders in m_q , we have decided to use consistently a linear ansatz for all contributions. We emphasize that this is equivalent to a quadratic ansatz in $M_N(m_q)$, since the Feynman-Hellmann theorem yields $\partial M_N / \partial m_q(m_{ud}) = \langle P | \bar{u}u + \bar{d}d | P \rangle$.

The results of the extrapolations are collected in tab.3. Note that the ratio of disconnected to connected contributions at the light quark mass is smaller than the values found in previous quenched simulations[4]. We find

$$\frac{\langle P | \bar{u}u + \bar{d}d | P \rangle_{disc}}{\langle P | \bar{u}u + \bar{d}d | P \rangle_{con}} = \frac{2D_q}{C_u + C_d} = 1.26(57) , \quad (19)$$

which differs appreciably from the quenched result[4] $2D_q/(C_u + C_d) = 2.23(52)$. We

Method	κ	D_q	D_s
SUM	0.1560	0.86(54)	0.79(54)
	0.1565	1.76(76)	1.74(74)
	0.1570	3.22(1.68)	3.19(1.61)
	0.1575	2.09(1.64)	1.85(1.44)
PAM	0.1560	1.63(37)	1.52(35)
	0.1565	1.49(45)	1.52(44)
	0.1570	1.67(71)	1.64(68)
	0.1575	2.68(93)	2.49(86)

Table 2: *Lattice results (unrenormalised) of the disconnected amplitudes $D_q = \langle P(\kappa_{sea}) | \bar{q}q(\kappa_{sea}) | P(\kappa_{sea}) \rangle_{dis}$ and $D_s = \langle P(\kappa_{sea}) | \bar{q}q(\kappa_{str}) | P(\kappa_{sea}) \rangle_{dis}$. $\kappa_{str} = 0.15608$.*

Table 3: *Lattice results for connected and disconnected amplitudes at $\kappa_{light} = 0.158462$. We have used the data from the plateau method PAM for the connected and disconnected amplitudes respectively.*

C_u	C_d	$2D_q$	$C_u + C_d + 2D_q$
2.40(19)	1.53(15)	4.95(2.36)	8.82(2.52)

attribute this difference to the influence of sea quarks in our full QCD simulation.

As a cross check we compare the total value $C_u + C_d + 2D_q = 8.82(2.52)$ with our result from the quadratic extrapolation of the nucleon mass[8]

$$\frac{\partial M_N}{\partial m_q}(m_{ud}) = 11.7(4.9) , \quad (20)$$

and find agreement. Note that the statistical uncertainty of the total amplitude obtained with the direct (ratio) method is smaller than the one from the derivative method (29% compared to 42%).

Finally, we determine the pion-nucleon σ -term in physical units. With³ $m_l = 0.000901(54)$ and $a_\rho^{-1} = 2.30 \text{ GeV}$ [8] one obtains

$$\sigma_{\pi N} = a_\rho^{-1} m_{ud} \langle P | \bar{u}u + \bar{d}d | P \rangle = 18(5) \text{ MeV} . \quad (21)$$

The statistical error has been determined with a full jackknife analysis of the product, including the jackknife distributions of m_{ud} and a_ρ^{-1} .

³We use the standard definition of the quark mass $m_q = \frac{1}{2}(\frac{1}{\kappa} - \frac{1}{\kappa_c})$.

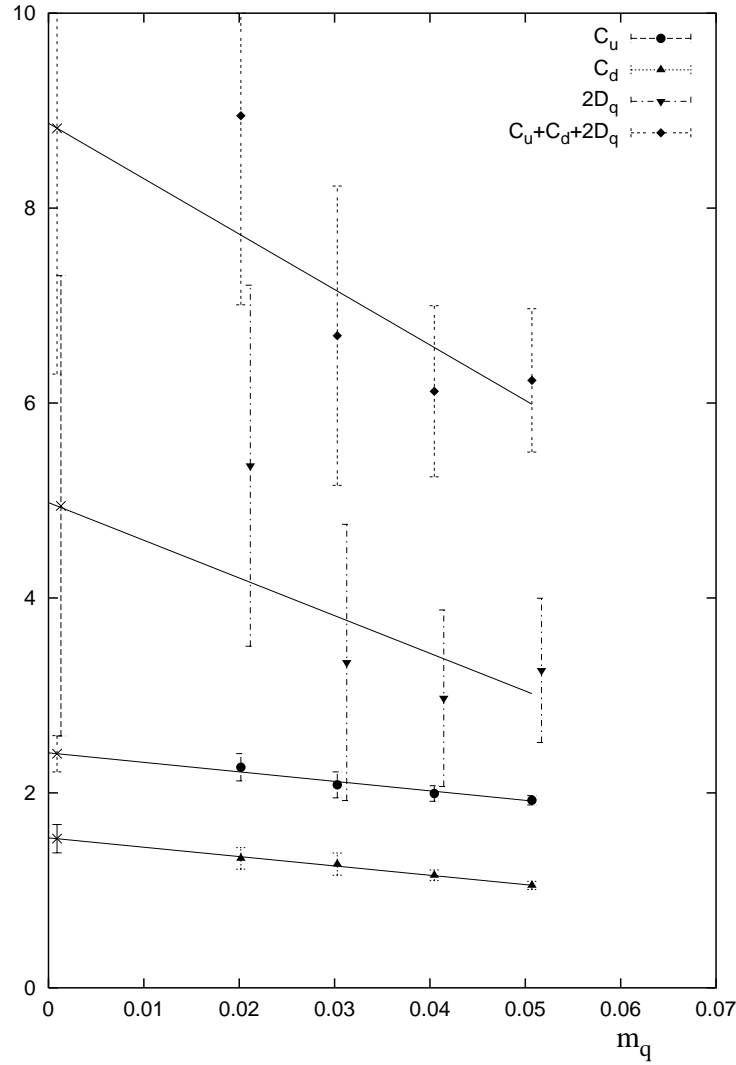


Figure 6: *Linear extrapolation of connected and disconnected amplitudes to the light quark mass. Bursts indicate the results of the extrapolation.*

Clearly, this is a rather small value, compared to the estimate from experiment. The latter is quoted to be $\sigma_{\pi N} \simeq 45$ MeV, which by the way is in rough agreement with quenched lattice estimates. To trace the mechanism behind, we follow the numbers in terms of amplitude and quark mass in comparison to the respective quenched predictions, ref.[4]⁴. In doing so, we carry out the necessary renormalizations – in accord with ref.[4] – by use

⁴We do not compare with the quenched results of ref.[5] since in this work the chiral extrapolation has been done in a different way.

of the tadpole improved renormalization factor[15]

$$Z_S = \frac{1}{2\kappa} \left(1 - \frac{3\kappa}{4\kappa_c}\right) \left[1 - 0.0098\alpha_{\bar{MS}}\left(\frac{1}{a}\right)\right], \quad (22)$$

where $\alpha_{\bar{MS}}\left(\frac{1}{a}\right) = 0.215$.

	$Z_S(C_u + C_d)$	$Z_S(2D_q)$	sum	$Z_S^{-1}m_la^{-1}[\text{MeV}]$
ref.[4] quenched	2.62(6)	5.8(1.4)	8.6(1.4)	5.0(2)
this work $n_f = 2$	3.11(25)	3.9(1.8)	7.0(2.0)	2.7(2)[16]

Table 4: *Compilation of renormalised results at the light quark mass.*

The numbers are collected in tab.4: Unquenching tends to enhance the connected part of the amplitude and dampen the disconnected contribution, yet the effects are indicative only, considering the size of statistical errors. Note that the origin for the apparent dramatic unquenching effect on $\sigma_{\pi N}$ can be traced directly to the substantial drop (roughly by a factor 1/2) observed in the light quark mass, m_{ud} [16].

Gupta has reasoned in the context of his discussion on light quark masses[17] that the validity of the one loop formula, eq.22, is questionable in full QCD, insofar large non perturbative contributions due to the presence of sea quarks could arise and readily change $Z_m = Z_S^{-1}$ by a factor of two, thus compensating the above factor 1/2 in m_{ud} . However, this doubt does not provide a source for a possible underestimate to $\sigma_{\pi N}$, since we are dealing here with a renormalization group invariant quantity.

On the other hand, one might question the standard definition and switch to the lattice quark mass as defined by use of the axial vector Ward identity[17, 20, 21]. But from the final analysis of the CP-PACS group on quenched QCD reported recently [21] one would gather a *decrease* of m_{ud} and $\sigma_{\pi N}$ by 20 – 50%! One should remember, though, that both definitions of m_{ud} differ at our value of a equally from their common continuum limit, and it is thus not a priori obvious which one of them is more suitable.

Obviously the only way to decide on this issue is to perform a scaling analysis of m_{ud} , i.e. to repeat its calculation at several lattice cutoffs a^{-1} , and then to extrapolate to the continuum $a \rightarrow 0$. We mention that the CP-PACS collaboration has launched such a scaling study in full QCD, based on three different values of the cutoff[19]. Their very preliminary analysis strongly hints at a *small value* of the light quark mass in the continuum limit, which incidentally is close to the estimate underlying our present work[16].

4.2 y Parameter

The determination of the y parameter, defined in eq.3, requires the calculation of the (purely disconnected) matrix element $\langle N|\bar{s}s|N\rangle$. In principle, a fully consistent QCD lattice analysis of this quantity can be done only in the setting of a realistic $n_f \geq 3$ simulation, in which strange and light quarks enter the dynamics through the fermion determinant.

Given our $n_f = 2$ setup, we can only resort to a semi-quenched analysis of the strange sector. This is done by identifying the masses of the sea quarks with those of the light valence quarks of the nucleon. The mass of the strange quark, which has no counterpart in the sea, is contained to match the strange hadron spectrum in semi-quenched analysis[8]. This procedure accounts at least for the influence of light sea quarks on the above matrix element and is certainly more adequate than previous quenched ($n_f = 0$) calculations.

The lattice raw results $D_s = \langle P(\kappa_{sea})|\bar{s}s](\kappa_s)|P(\kappa_{sea})\rangle$ are listed in tab.2. The values differ only slightly from the raw data D_q , indicating that an approximate $SU(3)$ flavour invariance of the disconnected contributions is still realised in our $n_f = 2$ simulation.

We extrapolate D_s as a function of κ_{sea} linearly to the light quark mass. To obtain the y parameter we renormalise our result

$$2\langle P|\bar{s}s|P\rangle = 4.94(2.14) \quad (23)$$

by Z_s , eq.22. This yields

$$y = \frac{2Z_S(\kappa_s)\langle P|\bar{s}s|P\rangle}{Z_s(\kappa_l)\langle P|\bar{u}u + \bar{d}d|P\rangle} = 0.59(13) . \quad (24)$$

Note that this is slightly lower than what was found with reliable statistics and comparable analysis methods in the quenched case [4]. The difference is almost entirely due to the fact that our ratio of disconnected to connected contributions, eq.19, is smaller.

It has been suggested by Lagaë and Liu [18] that the lattice quark mass dependent part of the renormalization factor would be quite different for connected and disconnected amplitudes. According to their reasoning, based on first order lattice perturbation theory, they would lower our value of y by about 30%. We do however not agree with their arguments, at least in the case of scalar quark loops, for the following reason: Since the combination $m_q\langle P|\bar{q}q|P\rangle$ is a renormalization group invariant quantity, both contributions to the amplitude, connected *and* disconnected, will be renormalised equally, i.e. by one and the same factor $Z_S = 1/Z_m$, where Z_m renormalises the quark mass. Choosing different factors, $Z_S^{con} \neq Z_S^{disc}$, as they propose, would be in conflict with the renormalisation group invariance.

5 Summary and Conclusions

We have studied connected and disconnected contributions to the proton scalar density amplitude in a $n_f = 2$ full QCD simulation at fixed lattice cutoff and volume.

It turns out that conventional ratio methods (summation and plateau) yield excellent signals for the connected parts, but fail in the determination of disconnected contributions. The latter situation can be improved substantially by use of PAM. It is likely that stochastic estimator techniques will perform even better on larger lattices, where we would expect self averaging effects to reduce the errors from the preset level, which is 30 - 40%.

We find the ratio of disconnected to connected contributions at m_{ud} to be lower than in quenched simulations. This provides first evidence for the influence of sea quarks on scalar density matrix elements. A definitive conclusion however would require a much higher statistical precision.

Due to the small value of m_{ud} in full QCD, the physical result for the pion-nucleon σ -term comes out rather low. It remains to be seen whether this is a finite cutoff effect. In this context it is very interesting that the preliminary results of the CP-PACS collaboration[19], obtained in full QCD with an improved action, point at an increase of m_{ud} by about 30% when changing from the standard to the Ward identity definition, at our value of a . It is obvious that a scaling analysis of the quark mass in full QCD is of utmost importance.

The y parameter has been determined in the framework of a semi-quenched analysis. The result $y = 0.59(13)$ is slightly closer to the phenomenological expectation than the value of a previous quenched simulation, performed with comparable analysis and extrapolation methods. This indicates the importance of sea quark contributions to this quantity. A full QCD calculation of y with $n_f \geq 3$ dynamical flavours is therefore highly desirable.

Acknowledgments We thank G. Ritzenhöfer for his contributions during the initial stage of this analysis. This work has been supported by the DFG grants Schi 257/1-4, 257/3-2, 257/3-3 and by the DFG Graduiertenkolleg "Feldtheoretische Methoden in der Statistischen und Elementarteilchenphysik". The connected contributions have been computed on the CRAY T3E systems of ZAM at FJZ. The disconnected parts were calculated on the APE100 computers at IfH Zeuthen and on the Quadrics machine provided by the DFG to the Schwerpunkt "Dynamische Fermionen", operated by the University of Bielefeld. We thank the staffs of these institutions for their kind support.

References

- [1] J. Gasser, H. Leutwyler, and M.E. Sainio Phys. Lett. B253(1991)252; Phys. Lett. B253 (1991)260.
- [2] B. Borasoy and U.G. Meißner, Phys. Lett. B365 (1996)285; V. Bernard, N. Kaiser, and U.G. Meißner, Phys. Lett.B389 (1996) 144.
- [3] J. Gasser, Ann. Phys. (NY) 136 (1981)61.
- [4] M. Fukugita, Y. Kuramashi, M. Okawa, and A. Ukawa, Phys. Rev. D51 (1995)5319.
- [5] S.J. Dong, J.F. Lagaë, and K.F. Liu, Phys. Rev. D54 (1996)5496; S.J. Dong, K.F. Liu, Nucl. Phys. B (Proc. Suppl.)42 (1995)322.

- [6] B. Altmeyer, M. Göckeler, R. Horsley, E. Laermann, and G. Schierholz, Nucl. Phys. B (Proc. Suppl.)34 (1994)376.
- [7] R. Gupta, C.F. Baillie, R.G. Brickner, G.W. Kilcup, A. Patel, and S.R. Sharpe, Phys. Rev. D44 (1991)3272.
- [8] SESAM Collaboration, N. Eicker, U. Glässner, S. Güsken, H. Hoeber, P. Lacock, T. Lippert, K. Schilling, A. Spitz, T. Struckmann, P. Ueberholz, and J. Viehoff, preprint HLRZ 1998-25, WUB 98-21, hep-lat 9896027, submitted to Phys. Rev. D.
- [9] L. Maiani, G. Martinelli, M.L. Paciello, and B. Taglienti, Nucl. Phys. B293 (1987)420.
- [10] G. Martinelli and C.T. Sachrajda, Nucl. Phys. B316 (1989)355.
- [11] M. Fukugita, Y. Kuramashi, M. Okawa, and A. Ukawa, Phys. Rev. D51 (1995)5319.
- [12] K. Bitar, A.D. Kennedy, R. Horsley, S. Meyer, and P. Rossi, Nucl. Phys. B313 (1989)348.
- [13] S.J. Dong and K.F. Liu, Nucl. Phys. B(Proc. Suppl.)26 (1992)353.
- [14] SESAM collaboration, N. Eicker, U. Glässner, S. Güsken, H. Hoeber, T. Lippert, G. Ritzenhfer, K. Schilling, G. Siegert, A. Spitz, P. Ueberholz, and J. Viehoff, Phys. Lett. B389 (1996)720.
- [15] G.P. Lepage and P.B. Mackenzie, Phys. Rev. D48(1993)2250.
- [16] SESAM Collaboration, N. Eicker, U. Glässner, S. Güsken, H. Hoeber, P. Lacock, T. Lippert, G. Ritzenhfer, K. Schilling, G. Siegert, A. Spitz, P. Ueberholz, J. Viehoff, Phys. Lett. B407(1997)290.
- [17] T. Bhattacharya and R. Gupta, Nucl. Phys. B (Proc. Suppl.) 63A-C (1998)95.
- [18] J.F. Lagaë and K.F. Liu, Phys. Rev. D52 (1995)4042; Nucl. Phys. B (Proc. Suppl.)42 (1995)355.
- [19] CP-PACS Collaboration, R. Burkhalter et al., Nucl. Phys. B (Proc. Suppl.) (1999), to appear.
- [20] V. Gimenez, L. Giusti, F. Rapuano, and M. Talevi, hep-lat/98010228.
- [21] CP-PACS Collaboration: S. Aoki et al., Nucl. Phys. B (Proc. Suppl.) (1999), to appear.